**Frontiers** | Frontiers in Biomaterials Science

# Injured nerves respond favorably to an integrated tension- and conduit-based regenerative strategy

Ting-Hsien Chuang[1], Elisabeth Orozco[1,2], Jae Jun Nam[1], Kenneth Vaz[1], Richard M. Lovering[3] and Sameer B. Shah[1,2,4]*

[1]Department of Orthopaedic Surgery, University of California, San Diego, La Jolla, CA, United States, [2]Research Service, VA San Diego Medical Center, San Diego, CA, United States, [3]Department of Orthopaedics, University of Maryland School of Medicine, Baltimore, MD, United States, [4]Department of Bioengineering, University of California, San Diego, La Jolla, CA, United States

**Introduction:** Numerous synthetic, hybrid, and biological grafts and conduits have been deployed to facilitate axonal regeneration across peripheral nerve gaps. Though some strategies have showed promise, larger gaps continue to be an unsolved clinical challenge. Recent evidence suggests that tension-based strategies offer a promising alternative approach to nerve repair. However, whether and to what degree severed peripheral nerves tolerate and accommodate tension, especially in the critical early stages of intervention, is less clear.

**Methods:** In this study, we evaluated a number of immuno-histochemical outcomes to test the hypothesis that injured rat sciatic nerves accommodate strains of up to 20%, a deformation magnitude that exceeds oft-quoted thresholds for nerve damage. We also assessed the possibility of integrating tension with conduit-based approaches for nerve repair.

**Results and Discussion:** There were no deficits in axonal, basal laminar, or extracellular matrix morphology with tension, though proximal and distal stumps of nerves in all experimental groups displayed abnormal morphology in proximity to the site of injury. Axons of stretched nerves successfully grew through guidance conduits into the distal stump within 6 weeks of repair, thus demonstrating the feasibility of combining tension- and conduit-based regenerative strategies.

## Introduction

Traumatic peripheral nerve injuries are a debilitating clinical challenge, resulting in motor dysfunction, sensory loss, and chronic pain. For transected nerves, end-to-end repairs lead to superior clinical outcomes compared to graft-based repairs (Millesi, 1986; Garg et al., 2021). However, excess tension at the repair site can result in nerve damage and catastrophic repair failure (Maeda et al., 1999; Sunderland et al., 2004). Given this concern, surgeons typically use a graft to repair larger (>1 cm) nerve gaps (Grinsell and Keating, 2014; Singh et al., 2022). Autologous grafts (autografts) are the current gold standard for repairing such gaps, but are limited by donor site morbidity, neuroma, geometric mismatch of the graft with proximal and distal nerve stumps, and limitations on

the length and viability of grafts that can be harvested (Schmidt and Leach, 2003; Meek et al., 2005; Selim et al., 2022). Furthermore, autograft efficacy is markedly decreased for gaps >3 cm (Selim et al., 2022).

Most alternative strategies for treating severe nerve injury involve the engineering of synthetic, biological, or hybrid conduits or grafts of increasing elegance and complexity [e.g., reviewed in (Schmidt and Leach, 2003; Li et al., 2021; Poongodi et al., 2021; de Assis et al., 2022; Selim et al., 2022)]. Such approaches have achieved clinical translation, with acellular human allografts deployed in increasing numbers of clinical trials and large-scale databases (Safa et al., 2020). On the other hand, grafts introduce additional length through which axons must grow before finally reaching the distal stump of the nerve (Brown et al., 2009; Bhatia et al., 2017), and though promising for some clinical settings (Rbia et al., 2019), allografts have not achieved autograft efficacy for all clinical contexts (Dunn et al., 2021; Peters et al., 2021). Thus, there remains a critical need for new regenerative strategies.

While not conventionally classified as "biomaterial-" or "graft-" based strategies," implantable and non-biological nerve-interfacing biomedical devices represent another approach to nerve regeneration. Peripheral nerve interfaces have long been implanted for neuromodulation or recording (Ray and Maurer, 1975). Correspondingly, neural stimulation principles have been integrated into regenerative technologies (Asri et al., 2022; Maeng et al., 2022). Though less typical, tension-based strategies have also been increasingly incorporated into biomedical devices for peripheral nerve repair. For short gaps, end-to-end repair under tension outperformed a tension-free autograft, based on functional and histological outcomes (Hentz et al., 1993; Sunderland et al., 2004; Howarth et al., 2019a), confirming that injured nerve stumps can accommodate tension if the repair can be protected (Kechele et al., 2011). For larger gaps, nerve-lengthening strategies have been used in rat, rabbit, and primate models. These strategies, which include modified external fixators and screw-based actuators (Beris et al., 1996; Arnaoutoglou et al., 2006; Saijilafu et al., 2006; Sharula et al., 2010; Yousef et al., 2015), have generally shown positive structural and functional outcomes. We built upon these studies by developing compact, implantable devices that draws the proximal stump linearly towards the distal stump to facilitate more distal nerve reattachment during a subsequent end-to-end repair surgery. This approach yielded comparable or superior outcomes to autografts (Chuang et al., 2013; Howarth et al., 2019b; Howarth et al., 2020).

Despite promising outcomes, tension-based regenerative approaches largely reflect empirical experimentation. Consequently, we lack insight into whether and to what degree severed peripheral nerves tolerate and accommodate tension, especially in the critical early stages of intervention (Abrams et al., 1998; Jiang et al., 2008). In this study, our primary intent was to test the hypothesis that nerves morphologically accommodates strains of up to 20%, a deformation magnitude that exceeds typically cited thresholds for nerve damage to vasculature or neural elements (Wall et al., 1992; Brown et al., 1993). In addition, we and others hypothesize that there may be benefits to concurrently integrating tension-based strategies with conduit-based solutions (Bazarek et al., 2022; Zeng et al., 2022). For example, a proximal stump could be stretched into a nerve gap and
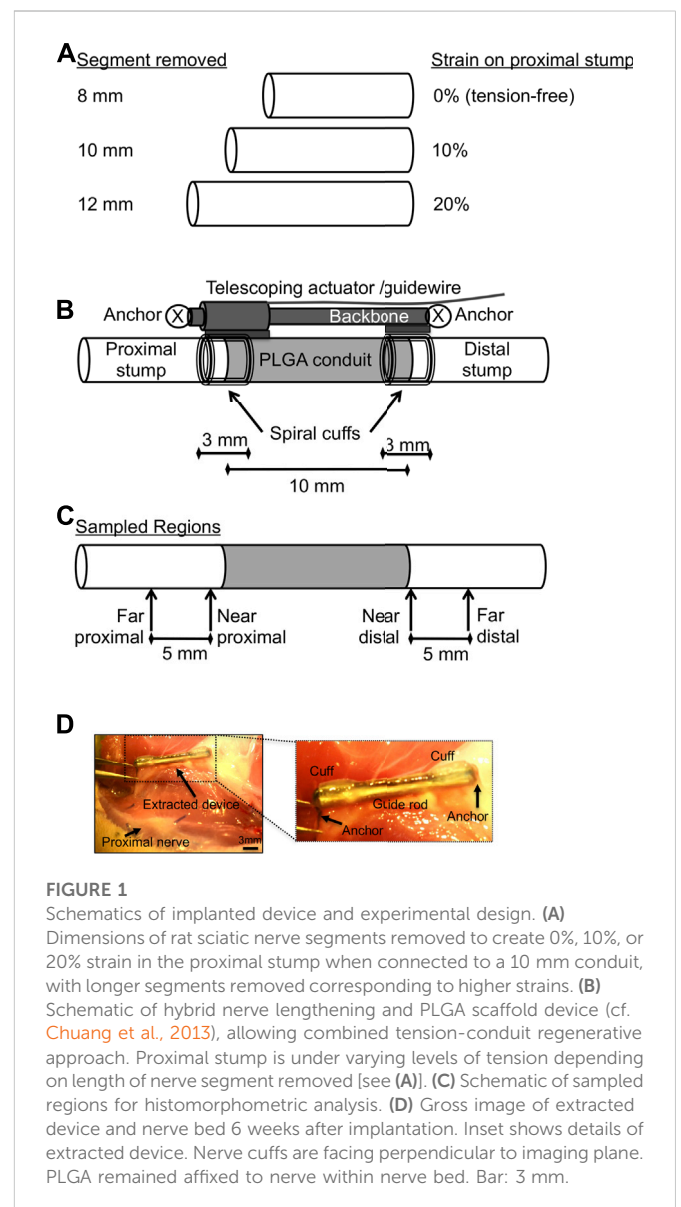


**FIGURE 1**
Schematics of implanted device and experimental design. **(A)** Dimensions of rat sciatic nerve segments removed to create 0%, 10%, or 20% strain in the proximal stump when connected to a 10 mm conduit, with longer segments removed corresponding to higher strains. **(B)** Schematic of hybrid nerve lengthening and PLGA scaffold device (cf. Chuang et al., 2013), allowing combined tension-conduit regenerative approach. Proximal stump is under varying levels of tension depending on length of nerve segment removed [see **(A)**]. **(C)** Schematic of sampled regions for histomorphometric analysis. **(D)** Gross image of extracted device and nerve bed 6 weeks after implantation. Inset shows details of extracted device. Nerve cuffs are facing perpendicular to imaging plane. PLGA remained affixed to nerve within nerve bed. Bar: 3 mm.

connected into a conduit, thereby reducing both the effective gap length to be bridged and required conduit material compared to standard tension-free conduits. Thus, a secondary goal of this study was to evaluate the feasibility of a combined tension-conduit based approach.

# Materials and methods

## Animals

Animal use was approved by the UCSD Institutional Animal Care and Use Committee. Adult male Sprague Dawley rats 12 weeks of age (350–400 g) were used. Due to observed autotomy in our initial cohort of Sprague-Dawley rats (Carr et al., 1992), Lewis rats (N = 2–3 group) of the same age were also used in a subsequent cohort; there were no apparent difference in any measured outcomes (excepting autotomy) across strain, and so data were pooled between strains. A cohort of age-matched controls was also used to provide a frame of reference for

parameter values in injured nerves; this avoided any impacts of altered loading on contralateral control limbs.

## Nerve injury and device implantation

Sciatic nerve gaps were induced as previously published in a manuscript detailing methods of nerve injury, device fabrication, and device implantation (Chuang et al., 2013). Briefly, anesthesia was induced under 5% isoflurane, followed by subcutaneous injection of analgesic (0.05 mg/kg buprenorphine) and antibiotics (5 mg/kg Baytril®), and the nerve exposed by separating heads of the biceps femoris. With the hip, knee, and ankle in a neutral position, an 8, 10, or 12 mm segment of sciatic nerve was excised proximal to its trifurcation, to create strains of 0%, ~10%, and ~20% after device implantation (Figure 1A), which imposed a gap of 10 mm between the tips of the proximal and distal stump (Figure 1B). Strains on the proximal stump were calculated based on the change of spacing between two painted epineurial markers just proximal to the cuffed region, before and after device implantation (Foran et al., 2017).

Implanted devices were slightly modified from our original devices [Figure 1B; cf. Figure 5 in (Chuang et al., 2013)]. Briefly, devices consisted of self-sizing silicone spiral nerve cuffs ~0.85 mm in diameter [cf. Figure 2 in (Chuang et al., 2013)], a telescoping backbone (14-gauge stainless steel hypotube upon a stainless steel rod 1.57 mm in diameter) to which the cuffs are attached, and 28-gauge steel wire anchors to secure the device to the underlying nerve bed. Nerve cuffs grasped both nerve stumps, while also distributing clamping loads during proximal stump tensioning. A poly(lactic co-glycolic) acid (PLGA) nerve guidance channel [NGC, cf. Figure 3 in (Chuang et al., 2013)] with inner diameter of ~1.2–1.6 mm, wall thickness of 0.3–0.4 mm, and length as specified in Figure 1, was also integrated into each device, just distal to the proximal cuff (Chuang et al., 2013). NGC dimensions allowed the nerve to rest within its lumen, without compression. All components were affixed to the device backbone using medical grade n-butyl cyanoacrylate adhesive (Chuang et al., 2013).

Devices were sterilized using ethylene oxide before use. The backbone of the device was positioned along the original axis of the nerve and anchored to the underlying muscle using 28-gauge steel wire. Proximal and distal nerve stumps were secured in cuffs and in NGC groups, the tips of the nerve stumps were carefully brought to the opening of PLGA NGC by manipulating the epineurium [cf. Figure 5 in (Chuang et al., 2013)].

For all animals, anesthesia was maintained at 2%–2.5% isoflurane throughout the surgery. After device implantation, the incision to muscle and skin were closed by 4-0 Vicryl® suture and 3-0 Prolene® monofilament suture, respectively. Rats were provided analgesics and full access to food and water post-op. The quality of device implantations was visually confirmed by an orthopaedic surgeon.

## Histological sample preparation

Rats were euthanized via CO₂ 3 or 6 weeks after surgery, to evaluate axonal outgrowth and nerve histomorphometry at early time points after repair. At the terminal time point, the implanted device was retrieved along with at least 8 mm of each nerve stump. After noting cuffed regions, nerves were released from the device, pinned on cork at slack length, and snap-frozen in liquid nitrogen-chilled isopentane. Prior to sectioning, segments of

**TABLE 1 Scheme for blind scoring of epineurial integrity and connective tissue infiltration based on trichrome staining.**

| Epineurial integrity |
| --- |
| 1. Perfect |
| 2. Intact interior border, fraying outer border |
| 3. Diffuse interior and exterior border, but still visible/dark |
| 4. Diffuse interior ands exterior border, less clear border |
| 5. No epineurium visible |
| **Intra-epineurial connective tissue density score** |
| 1. Perfectly clean/normal |
| 2. Slightly less compact inner structure, slight connective tissue |
| 3. Moderate inner structure, moderate connective tissue |
| 4. Heavy connective tissue, light/less organized inner structure |
| 5. Heavy connective tissue; no structural integrity |

A rating of 1 for each reflects best quality, and 5 reflects worst quality.

interest were embedded in Tissue-Tek® O.C.T. Compound (Sakura Finetek, Torrance, CA), and 10 μm cross-sectional slices, sectioned on a cryostat (CM3050S, Leica, Buffalo Grove, IL), were mounted on a glass slide. Cross sections were obtained from 4 regions along the nerve (Figure 1C): 1) far proximal stump (~10 mm proximal to the nerve gap); 2) near proximal stump (within the cuff, ~3 mm proximal to the nerve gap); 3) near distal stump (within the cuff, ~3 mm distal to the nerve gap); 4) far distal stump (~10 mm distal to the original nerve gap).

## Immunohistochemistry (IHC), imaging, and image processing

To evaluate degeneration and regeneration of severed nerve stumps, the following primary antibodies, with appropriate anti-mouse or anti-rabbit Alexa Fluor®-488 or -594 conjugated secondary antibodies (Invitrogen, Carlsbad, CA), were used: mouse monoclonal anti-rat SMI31 (phosphorylated neurofilament) antibody (Abcam ab24573, Cambridge, MA); rabbit polyclonal anti-laminin antibody (Sigma L9393, St. Louis, MO); mouse monoclonal anti-CD68 (pan-macrophage; Abcam ab31630, Cambridge, MA). All antibodies were diluted 1:200. In addition, Masson's Trichrome stain (Poly Scientific, Bay Shore, NY) was used to identify connective tissue localization. Labeled slides were visualized using a Leica TCS SP5 confocal microscope (Leica microsystems, Buffalo Grove, IL) under 10x/0.6 and 63x/1.4 objectives with excitation and emission filters appropriate for desired fluorophores.

For axon counts and macrophage number, 10x images of SMI 31 antibody-labeled sections were converted to 8-bit binary images in ImageJ (v1.47; NIH, Bethesda, MD), thresholded using Otsu's method, and calculated using the "Analyze particles" function following removal of all objects less than 4 pixels as well as large structures such as blood vessels and artifactual labeling at the nerve periphery. Axonal and macrophage density was calculated by dividing the axon or macrophage counts by the cross-sectional area of the intra-epineurial region of the nerve, excluding major blood vessels. For axon diameter measurements, two randomly selected 63x confocal images of SMI31-
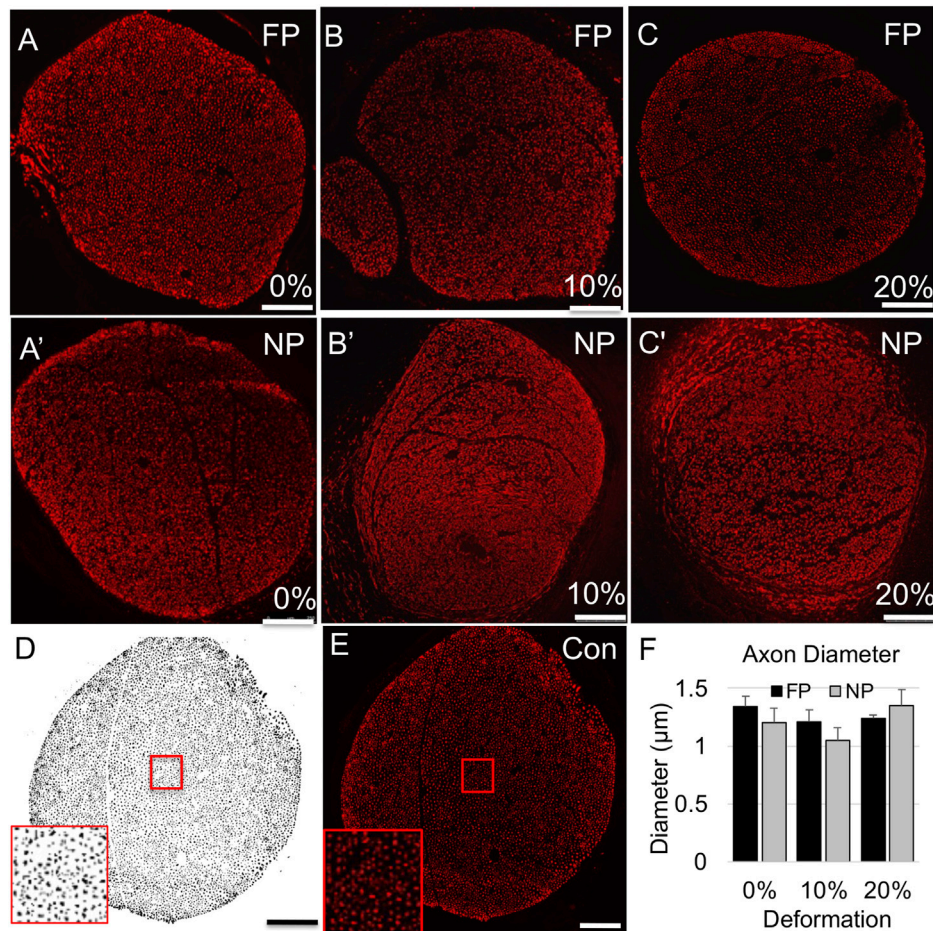
**FIGURE 2**
Axonal (SMI-31) immunolabeling in proximal stump. **(A–C)** Representative confocal images of axonal immunolabeling in far proximal stump in nerves stretched **(A)** 0%; **(B)** 10%; and **(C)** 20%. **(A′–C′)** Representative confocal images of axonal immunolabeling in near proximal stump in nerves stretched **(A′)** 0%; **(B′)** 10%; and **(C′)** 20%. **(D)** Sample binary image used to quantify axonal parameters. **(E)** Contralateral control nerve. Insets in **(D,E)** show that individual axons can be clearly resolved. Scale bars: 100 μm. **(F)** Axon diameters are not significantly affected by region or deformation. Additional outcomes and comprehensive statistical analysis are presented in Table 2.

labeled nerves were thresholded using Otsu's method and processed using a custom MATLAB algorithm (MathWorks, Natick, MA) based on pixels per object. Basal lamina integrity was evaluated from 63x confocal images of laminin antibody-labeled slides. To quantify connectivity and integrity of the basal lamina, we converted 63x images of laminin-labeled nerves to a binary image using Otsu's method following application of a Gaussian smoothing filter (radius 3) on the raw image, to reduce high-frequency noise. Laminin area fraction was calculated as a measure of the overall presence of basal lamina. Laminar compaction was assessed by manually quantifying the ratio of open laminar objects (uncompacted) to total laminar objects ($n > 80$/section). Connective tissue infiltration and integrity were scored using criteria in Table 1, slightly modified from (Foran et al., 2017).

## Statistics

Mean parameters among device implantation groups were compared using mixed two-way ANOVA to test effects of region (a repeated measure) and strain. Post hoc comparisons were made using Sidak's test, which accounts for multiple comparisons. Dunnett's test was used to compare far proximal regions at each strain to control values. A minimum sample size of 4 animals per group was required to achieve a power of 0.85 and type I error α of 0.05, given effect sizes of 0.45 calculated using Cohen's d based on pilot ($n = 3$) means and standard deviations of macrophage density. Power calculations were performed using G*Power 3.1 (Faul et al., 2007). To be conservative, 5–7 samples per group were analyzed. The variability in sample size within a group resulted from early euthanasia required in some groups due to self-mutilation noted above. $n = 7$ device implantations were performed for 10% and 20% strain at the 3 weeks time point, $n = 6$ for 0% strain at the 3 weeks time point, and $n = 5$ for each strain at the 6 weeks time point.

## Results

### Device implantation

We bridged a 10 mm nerve gap following successful device implantation that resulted in a 0% (0.0 ± 0.0), ~10% (10.2 ± 0.3%),

TABLE 2 Summary of mean morphological parameters in proximal stump (Mean+/−SEM).

| Parameter | S/R | FP/NP | 0% | 10% | 20% |
|---|---|---|---|---|---|
| Axon number (#) | — | FP | 5218 ± 661 | 6446 ± 1,290 | 5491 ± 353 |
| | | NP | 5064 ± 770 | 5341 ± 556 | 4626 ± 812 |
| Axon density (#/$\mu m^2$) | R | FP | $5 \times 10^{-3} \pm 4 \times 10^{-4}$ | $6 \times 10^{-3} \pm 5 \times 10^{-4}$ | $7 \times 10^{-3} \pm 7 \times 10^{-4}$ |
| | | NP | $5 \times 10^{-3} \pm 6 \times 10^{-4}$ | $6 \times 10^{-3} \pm 9 \times 10^{-4}$ | $5 \times 10^{-3} \pm 4 \times 10^{-4}$* |
| Axon diameter ($\mu m$) | — | FP | 1.34 ± 0.09 | 1.21 ± 0.10 | 1.24 ± 0.03 |
| | | NP | 1.20 ± 0.13 | 1.05 ± 0.11 | 1.35 ± 0.14 |
| Macrophage density (#/$\mu m^2$) | R | FP | $5 \times 10^{-5} \pm 2 \times 10^{-5}$ | $5 \times 10^{-6} \pm 1 \times 10^{-6}$ | $7 \times 10^{-6} \pm 2 \times 10^{-5}$ |
| | | NP | $3 \times 10^{-4} \pm 9 \times 10^{-5}$* | $6 \times 10^{-4} \pm 2 \times 10^{-4}$*# | $2 \times 10^{-4} \pm 7 \times 10^{-5}$* |
| Epineurial integrity score | R | FP | 1.2 ± 0.2 | 1.2 ± 0.2 | 1.4 ± 0.2 |
| | | NP | 3.0 ± 0.6* | 2.4 ± 0.2˜ | 3.6 ± 0.4* |
| Connective tissue infiltration score | R | FP | 1.0 ± 0.0 | 1.4 ± 0.2 | 1.4 ± 0.4 |
| | | NP | 3.0 ± 0.5* | 2.2 ± 0.2 | 2.8 ± 0.2* |
| Laminin area fraction (%) | | FP | 42.1 ± 5.0 | 41.3 ± 4.4 | 34.6 ± 6.1 |
| | | NP | 37.6 ± 4.8 | 35.7 ± 2.0 | 39.6 ± 7.3 |
| Open laminar tubes (%) | R | FP | 88.6 ± 2.3 | 87.0 ± 1.5 | 86.6 ± 2.2 |
| | | NP | 53.8 ± 3.7* | 54.0 ± 5.1* | 46.0 ± 3.1* |

S/R indicates significant effect of strain (S) and/or region (R) based on 2-way ANOVA. FP, Far proximal; NP, Near proximal. Based on Sidak post-hoc testing: * Significantly different from FP at same strain; ˜ Strongly trends towards different from FP at same strain ($p < 0.06$). # Significantly different from 20% strain in same region. All significant differences are $p < 0.05$, with exact significance indicated in results text.

or ~20% (20.2 ± 0.7%) strain in the proximal stump at a location just proximal to the cuffed nerve. The implanted device was retrieved cleanly after three and 6 weeks from within an overlying layer of loosely adherent connective tissue [Figure 1D; cf. Figure 6 in (Chuang et al., 2013)], and nerves were readily freed from cuffs and the PLGA scaffold for subsequent analysis. On the other hand, 27.8% of all Sprague-Dawley rats (5/18 total) exhibited significant autotomy of the injured limb and were euthanized before the 3-week endpoint. This behavior did not correlate with strain, as 33%, 16.7%, and 33% of animals in 0%, 10%, and 20% strain groups, respectively, were affected. Lewis rats did not exhibit autotomy, consistent with previous data (Carr et al., 1992).

## Proximal stump

We examined influences of tension on the regenerating proximal stump, both in intact but mechanically loaded (far proximal) regions, and newly regenerating (near proximal) regions of the proximal stump (Figure 1C). First, we assessed axonal number, density, and diameter based on immunolabeling of phosphorylated neurofilaments (Figure 2; Table 2). Two-way ANOVA indicated no effect of strain or region on axonal number or diameter, but a significant effect of region on axonal density ($p < 0.028$; Table 2). This regional difference manifest itself most prominently in the 20% strain group, in which far proximal stumps contained a significantly higher density of axons compared to the near proximal region ($p < 0.039$; Table 2). Axonal density and number in the far proximal (most intact) region were not

significantly different from control nerves (density: $p > 0.6$; number: $p > 0.5$); however, average axonal diameters for all three strains were significantly smaller than that of control nerves (1.65 ± 0.14; $p < 0.02$, Dunnett's test).

We then examined the influence of tension on the inflammatory response and structural environment of the proximal stump. Again, while there was no effect of tension on macrophage density ($p = 0.27$), a strong regional effect was observed ($p < 0.0005$). Increased macrophage infiltration was observed at the near proximal stump compared to the far proximal stump for all groups (Figure 3; Table 2), and significantly for the 10% strain group ($p < 0.003$, Sidak). Consistent with this result, blind scoring of epineurial integrity and intra-epineurial connective tissue infiltration revealed no effect of tension, but a significant effect of region on both epineurial integrity ($p < 0.0001$) and connective tissue infiltration ($p < 0.0002$; Figure 4; Tables 1, 2). At both 0% and 20% strain, post-hoc testing revealed decreased epineurial integrity (0%: $p < 0.006$; 10%: $p < 0.06$; 20%: $p < 0.001$; Sidak) and increased connective tissue infiltration (0%: $p < 0.002$; 20%: $p < 0.03$; Sidak) in near compared to far proximal regions. The far proximal stump also maintained superior integrity of the basal lamina compared to the near proximal stump. Laminin immunolabeling revealed that though area fractions were regionally similar, there was a significant effect of region on the fraction of open laminar tubes ($p < 0.0001$), with a higher fraction in far proximal compared to near proximal regions at all three strains ($p < 0.0001$ for all strains; Figure 5; Table 2). No
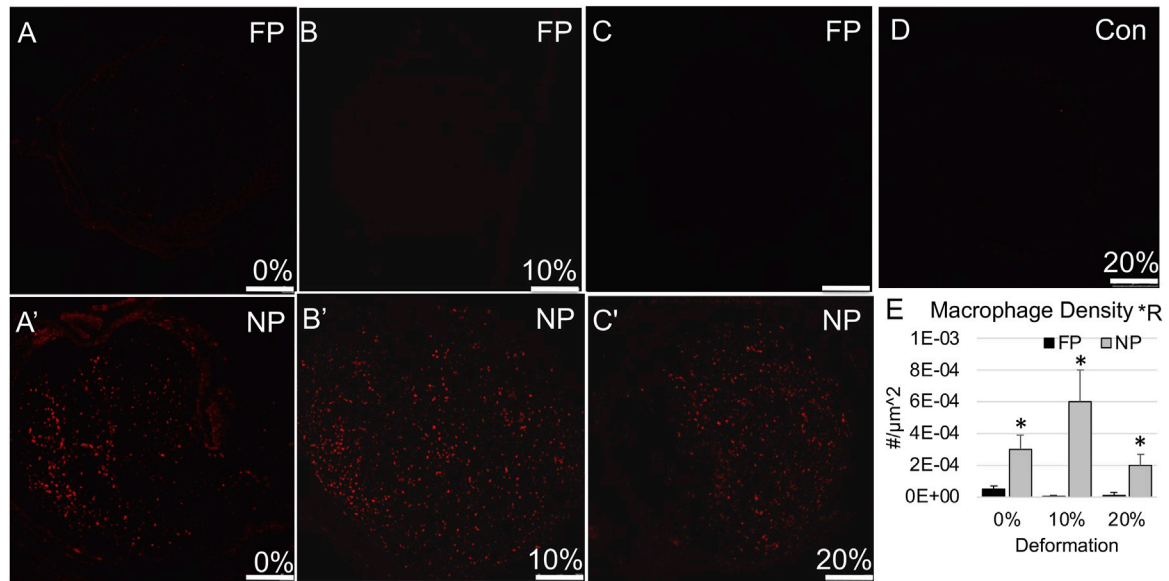
**FIGURE 3**
Macrophage (CD68) immunolabeling in proximal stump. **(A−C)** Representative confocal images show minimal CD68 immunolabeling in far proximal stump in nerves stretched **(A)** 0%; **(B)** 10%; and **(C)** 20%. **(A′−C′)** Representative confocal images show increased CD68 immunolabeling in near proximal stump in nerves stretched **(A′)** 0%; **(B′)** 10%; and **(C′)** 20%. **(D)** Contralateral control nerve. Scale bars: 250 μm. **(E)** Macrophage density is significantly affected by region (*R: $p < 0.05$, effect of region, 2-way ANOVA; *: $p < 0.05$, NP vs. FP), but not deformation with near proximal regions exhibiting a higher density. Additional outcomes and comprehensive statistical analysis are presented in Table 2.
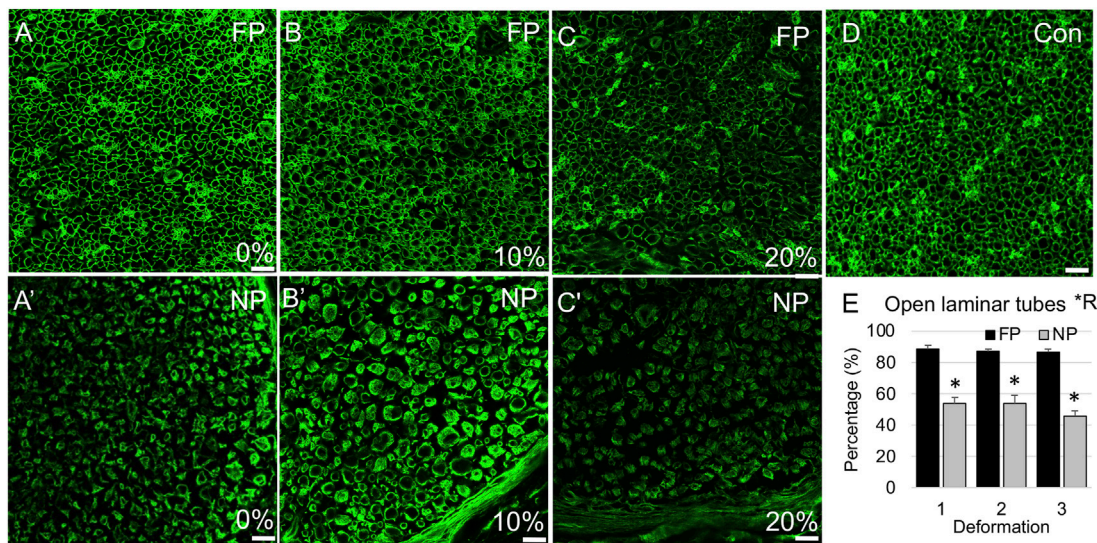


**FIGURE 4**
Laminin immunolabeling in proximal stump. **(A−C)** Representative confocal images of laminin immunolabeling show open laminar tubes in far proximal stump of nerves stretched **(A)** 0%; **(B)** 10%; and **(C)** 20%. **(A′−C′)** Representative confocal images of laminin immunolabeling show higher likelihood of compacted laminar tubes in near proximal stump of nerves stretched **(A′)** 0%; **(B′)** 10%; and **(C′)** 20%. **(D)** Contralateral control nerve. Scale bars: 20 μm. **(E)** The percentage of open laminar tubes is significantly affected by region (*R: $p < 0.05$, effect of region, 2-way ANOVA; *: $p < 0.05$, NP vs. FP), but not deformation, with near proximal regions exhibiting increased laminin remodeling and compaction. Additional outcomes and comprehensive statistical analysis are presented in Table 2.

significant differences were observed in macrophage density, epineurial integrity, connective tissue infiltration, or laminar integrity between the far proximal stump and contralateral control nerves.

## Distal stump

We also probed whether tension accelerated or suppressed degenerative outcomes in the distal stump, and whether the
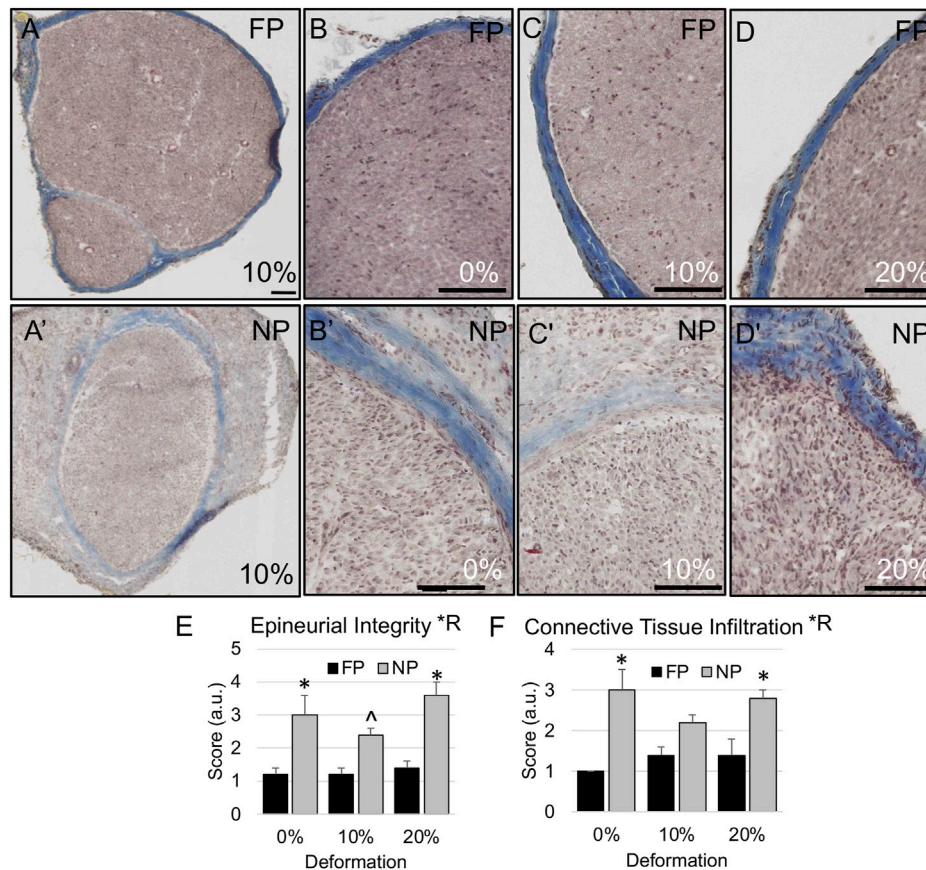
**FIGURE 5**
Epineurial integrity in proximal stump. **(A–D)** Representative trichrome-stained images of the nerve show intact epineurial boundaries in far proximal stump of nerves stretched **(B)** 0%; **(A,C)** 10%; and **(D)** 20%. **(A'–D')** Representative trichrome images show more diffuse epineurial borders in near proximal stump of nerves stretched **(B')** 0%; **(A',C')** 10%; and **(D')** 20%. Scale bars: 100 μm. **(E)** Epineurial integrity and **(F)** connective tissue infiltration are significantly affected by region (*R: $p < 0.05$, effect of region, 2-way ANOVA; *: $p < 0.05$, NP vs. FP; $p < 0.06$ [strong trend], NP vs. FP), but not deformation, with near proximal regions exhibiting reduced epineurial integrity and increased connective tissue infiltration into nerve fascicles. Additional outcomes and comprehensive statistical analysis are presented in Table 2.

structural response varied regionally. There were no effects of tension, favorable or unfavorable, on any inflammatory and morphological parameters in the distal stump. As was the case for the proximal stump, regions closer to the site of injury (near distal) experienced increased connective tissue infiltration and decreased laminar integrity compared to the far distal stump (Figures 6–8; Table 3). Though there were no regional effects on macrophage density ($p = 0.018$), there was a significant of region on epineurial integrity ($p < 0.0001$) connective tissue infiltration ($p < 0.0001$), and the proportion of open laminar tubes ($p < 0.0001$), as well as a strong trend towards differences in laminar area fraction ($p < 0.07$). Post hoc testing revealed significantly higher epineurial integrity (0%: $p < 0.005$; 10%: $p < 0.02$; 20%: $p < 0.02$, Sidak), lower connective tissue infiltration (0%: $p < 0.01$; 10%: $p < 0.004$; 20%: $p < 0.01$, Sidak), and more open laminar tubes (0%: $p < 0.0003$; 10%: $p < 0.03$; 20%: $p < 0.003$, Sidak) in far distal regions compared to near distal regions.

## Axonal outgrowth

Consistent with the lack of adverse effects of strain on axonal, structural, and inflammatory response in proximal or distal stumps, axons successfully regenerated halfway into the PLGA graft at 3 weeks in all three experimental groups, and into the distal stump at 6 weeks (Figure 9). An accurate quantitative evaluation of regenerative outgrowth was confounded by variability created by the unexpected partial flattening of some PLGA tubes in all three groups. Nevertheless, based on area fractions of regenerating axons within the guidance channels (3 weeks) and distal stumps (6 weeks), no apparent difference in structural regeneration was observed.

## Discussion

In this study, we addressed two questions from a morphological perspective: 1) whether tension affects the short-term regenerative response of severed nerves; 2) whether regional differences could be detected in the regenerative response in response to tension. In answering these questions, we also assessed the feasibility of tension-based regenerative strategies in combination with a nerve conduit. Our data indicate that tension did not impair
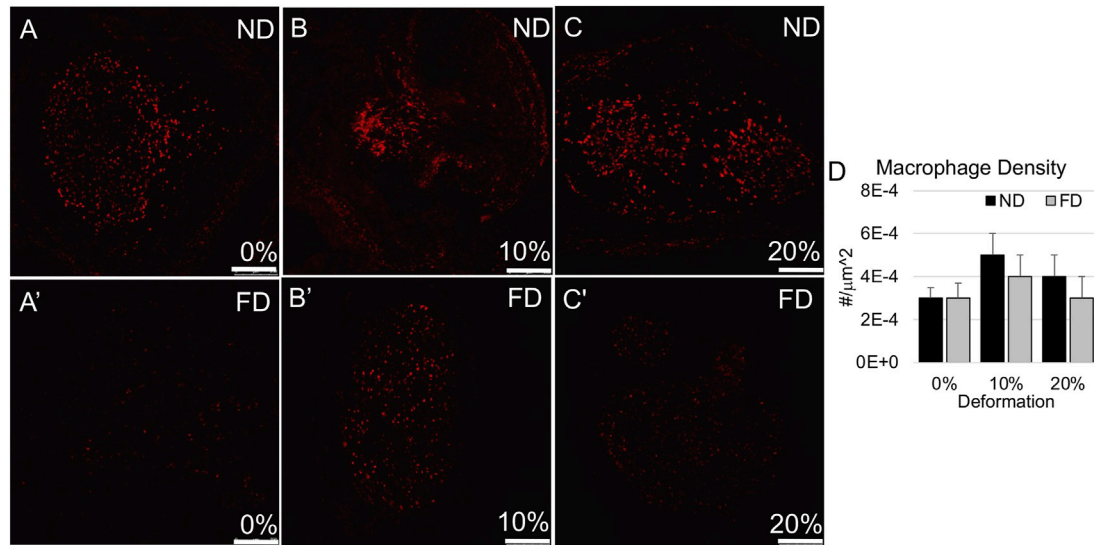
**FIGURE 6**
Macrophage (CD68) immunolabeling in distal stump. **(A–C)** Representative confocal images show modest levels of CD68 immunolabeling in near and far regions of the distal stump in nerves stretched **(A,A')** 0%; **(B,B')** 10%; and **(C,C')** 20%. Scale bars: 250 μm. **(D)** Macrophage density was not significantly affected by region or deformation within the distal stump. Additional outcomes and comprehensive statistical analysis are presented in Table 3.

**TABLE 3 Summary of mean morphological parameters in distal stump (Mean+/−SEM).**

| Parameter | S/R | ND/FD | 0% | 10% | 20% |
|---|---|---|---|---|---|
| Macrophage density (#/μm²) | — | ND | $3 \times 10^{-4} \pm 5 \times 10^{-5}$ | $5 \times 10^{-4} \pm 1 \times 10^{-4}$ | $4 \times 10^{-4} \pm 1 \times 10^{-4}$ |
| | | FD | $3 \times 10^{-4} \pm 7 \times 10^{-5}$ | $4 \times 10^{-4} \pm 1 \times 10^{-4}$ | $3 \times 10^{-4} \pm 1 \times 10^{-4}$ |
| Epineurial integrity | R | ND | 4.0 ± 0.3 | 4.2 ± 0.6 | 4.4 ± 0.4 |
| | | FD | 1.6 ± 0.2* | 2.2 ± 0.7* | 2.4 ± 0.6* |
| Connective tissue infiltration | R | ND | 3.6 ± 0.2 | 3.8 ± 0.6 | 4.0 ± 0.3 |
| | | FD | 2.4 ± 0.2* | 2.4 ± 0.5* | 2.8 ± 0.4* |
| Laminin area fraction | R˜ | ND | 35.4 ± 10.1 | 26.4 ± 5.1 | 19.8 ± 4.2 |
| | | FD | 33.1 ± 6.8 | 43.8 ± 4.9 | 32.7 ± 5.1 |
| Open laminar tubes (%) | R | ND | 34.6 ± 3.4 | 39.0 ± 2.8 | 34.6 ± 3.5 |
| | | FD | 55.5 ± 1.8* | 49.6 ± 1.9* | 49.4 ± 5.4* |

S/R indicates significant effect of strain (S) and/or region (R) based on 2-way ANOVA. R˜Strongly trends towards effect of region ($p < 0.07$) FP, Far proximal; NP, Near proximal. Based on Sidak posthoc testing: * Significantly different from ND at same strain. All significant differences are $p < 0.05$, with exact significance indicated in results text.

regenerative axonal outgrowth at strains up to 20%. Consistent with such growth, there were also no adverse effects of strains up to 20% on the morphology of axons, basal lamina, or extracellular matrix, suggesting that severed proximal nerve stumps can indeed tolerate and positively adapt to appreciable mechanical loads during regeneration (Figures 2–5, 9; Table 2). Imposition of tension also did not alter indicators of Wallerian degeneration in the distal stump (Figures 6–8; Table 3). Several interesting regional differences in structure were observed within regions of the nerve that appeared to be structurally intact, macroscopically. These differences could have important implications for the quality of the regenerative environment when pairing tension-based strategies with conduits or grafts.

## Effects of strain on regeneration of severed nerves

Like other tissues that span joints, peripheral nerves exist within a dynamic biomechanical environment. Excessive mechanical loading can profoundly impair peripheral nerve function, with strains above ~8%–12% typically associated with irreversible conduction deficits, structural damage, vascular ischemia, and formation of scar and adhesions (Lundborg and Rydevik, 1973; Millesi, 1981; Millesi, 1986; Ogata and Naito, 1986; Wall et al., 1992; Brown et al., 1993; Tanoue et al., 1996; Flores et al., 2000). On the other hand, during joint movement, nerves experience paradoxically high regional strains, in some cases approaching 30% (Wright et al., 2001). Such large deformations likely reflect regional differences in nerve structure
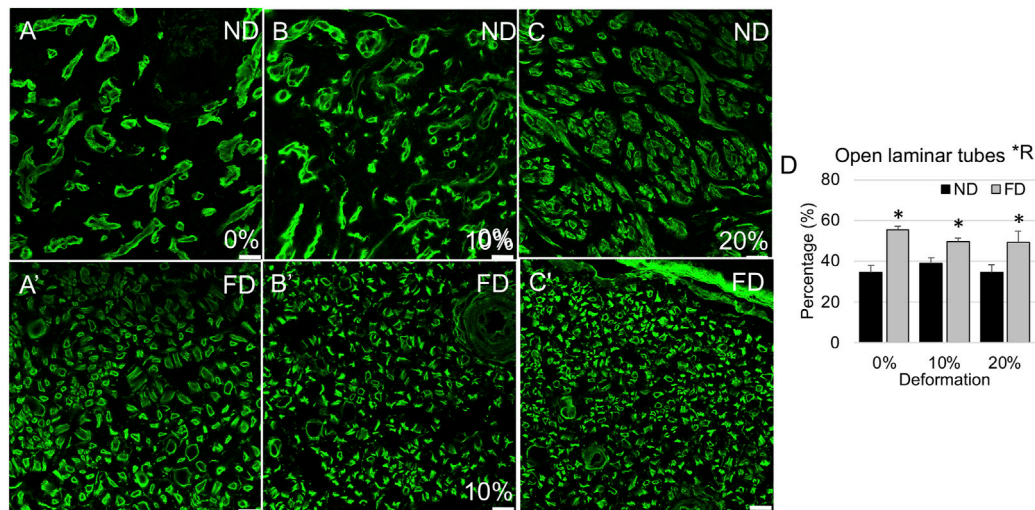
**FIGURE 7**
Laminin immunolabeling in distal stump. **(A–C)** Representative confocal images show laminar compaction in near distal stump in nerves stretched **(A)** 0%; **(B)** 10%; and **(C)** 20%. **(A'–C')** Representative confocal images show tubular laminar morphology in far distal stump in nerves stretched **(A')** 0%; **(B')** 10%; and **(C')** 20%. Scale bars: 20 μm. **(D)** The percentage of open laminar tubes is significantly affected by region (*R: $p < 0.05$, effect of region, 2-way ANOVA; *: $p < 0.05$, NP vs. FP), but not deformation, with near distal regions exhibiting increased laminin remodeling and compaction. Additional outcomes and comprehensive statistical analysis are presented in Table 3.

and biomechanical properties (Phillips et al., 2004; Mason and Phillips, 2011; Sung et al., 2019), and suggest that nerves can adapt to their mechanical environment (Mueller and Maluf, 2002). Consistent with this perspective, tension has been noted to promote neuronal growth, and is required for proper neuronal function and survival (Anava et al., 2009; Siechen et al., 2009). Cultured neurons also exhibit axonal tension under baseline conditions, and may be dramatically elongated in response to tensile loading, at rates exceeding those achieved by growth cone advancement (Bray, 1984; Dennerll et al., 1989; Zheng et al., 1991; Pfister et al., 2004). Axonal diameters and biological processes such as organelle and cytoskeletal transport are maintained or, in some cases, increased following stretch, suggesting an active structural and biological response to tension (Loverde et al., 2011; Bober et al., 2015). Similarly, at the tissue level, peripheral nerves accommodate physiological levels of lengthening during organism growth as well as imposed lengthening during surgical procedures such as limb-lengthening surgery (Birch and Samchukov, 2004; Simpson et al., 2013). Thus, there is substantial evidence that nerves respond favorably to moderate tension.

Several studies, including a modified version of our device, have demonstrated the feasibility of direct end-to-end repairs under tension (Hentz et al., 1993; Sunderland et al., 2004; Kechele et al., 2011; Howarth et al., 2019a). In addition, progressive lengthening over days to weeks followed by end-to-end repair also results in positive outcomes (Sharula et al., 2010; Hara et al., 2012; Howarth et al., 2019b; Howarth et al., 2020). However, beyond axonal densities and, occasionally, neuronal geometry, little quantification is provided on the morphological response to tension. Our data complement these studies by providing detailed morphological evidence supporting the absence of adverse effects of strains up to 20% on axonal number and quality as well as a consistent regenerative environment both proximal and distal to the injury site. There appears to be no downside to imposing deformation on proximal stumps exceeding oft-cited 8%–12%

levels thresholds for neural injury (Lundborg and Rydevik, 1973; Millesi, 1981; Millesi, 1986; Ogata and Naito, 1986; Wall et al., 1992; Brown et al., 1993; Tanoue et al., 1996; Flores et al., 2000). Maximum strains imposed in this study are similar to those experienced by rat nerves in joint configurations corresponding to maximum physiological strain (Foran et al., 2017). Methodologically, imposition of strains on nerves is enabled by gripping the nerve over a relatively large surface area, such that local stresses are likely to be distributed over this area. Such a feature is likely to protect the nerve from stress concentrations during loading and should be integrated into devices designed for clinical translation. Due to the encapsulation of the nerve and device during repair, it is not possible to assess the degree to which nerves have remodeled to relieve this tension. However, *in vitro* studies and examinations of uninjured nerves indicate consistency of axonal diameter and nerve function in response to deformation as well as increases in internodal distances (Pfister et al., 2004; Simpson et al., 2013; Loverde and Pfister, 2015). These observations demonstrate active longitudinal and radial growth of nerve fibers. In fact, the lack of adverse effects suggests that maximal thresholds for deformation may exceed 20%.

From a device design perspective, an important distinction between our approach and previous approaches is the use of nerve cuffs to redistribute tension. Suture pullout is cited as a possible mode of failure during nerve traction following reattachment of nerves and other tissues (Abrams et al., 1998; Jiang et al., 2008). In contrast, nerve cuffs are more likely to distribute local stress concentrations than sutures, and thereby more predictably and robustly accommodate strain.

## Regional differences in regenerative and degenerative environments

An important outcome of our study was the observation of dramatic regional differences within proximal and distal stumps (Figure 10). Far
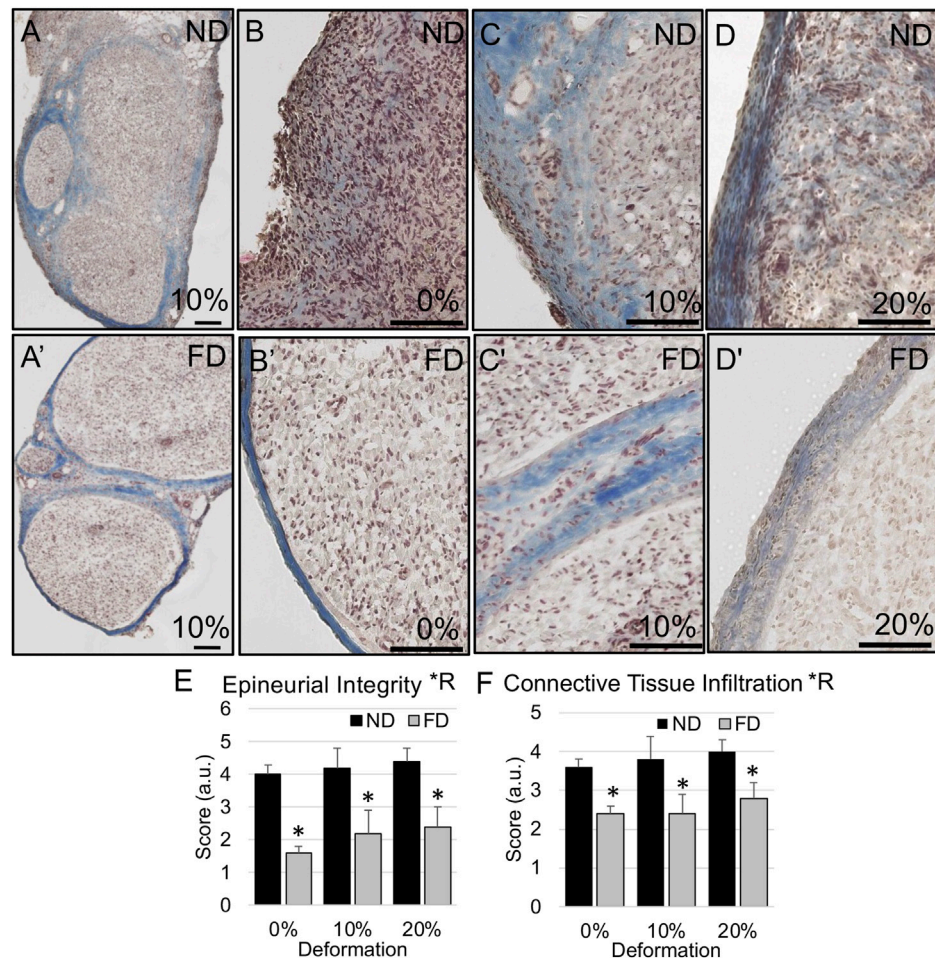
**FIGURE 8**
Epineurial integrity in distal stump. **(A–D)** Representative trichrome images show higher likelihood of diffuse epineurial borders in near distal stump of nerves stretched **(B)** 0%; **(A,C)** 10%; and **(D)** 20%. **(A'–D')** Representative trichrome images show intact epineurial boundaries in far distal stump of nerves stretched **(B')** 0%; **(A',C')** 10%; and **(D')** 20%. Scale bars: 100 μm. **(E)** Epineurial integrity and **(F)** connective tissue infiltration are significantly affected by region (*R: $p < 0.05$, effect of region, 2-way ANOVA; *: $p < 0.05$, NP vs. FP), but not deformation, with near distal regions exhibiting reduced epineurial integrity and increased connective tissue infiltration into nerve fascicles. Additional outcomes and comprehensive statistical analysis are presented in Table 3.

proximal (intact) regions of the "living" proximal stump were, as expected, similar in quality and composition to contralateral control nerves. Axon diameters in the proximal stump were slightly smaller for all three strains, likely secondary to the initial dying back following nerve transection (Geuna et al., 2009). However, the extracellular matrix and basal lamina maintained their integrity and there were no differences in axonal number and density. Uninjured, cuffed control nerves also showed no apparent changes to underlying structure, confirming that any observed regional differences were not an artifact of compressive neuropathy observed in response to implantation of thicker, larger cuffs (Gupta et al., 2004; Gupta et al., 2012).

Axon number trended lower in newly regenerated near proximal regions than far proximal regions suggesting that not all injured axons regenerate. This was also reflected in a significant effect of region on axonal density, in which the near proximal region exhibited significantly lower axonal density (Table 2). These effects on axonal quality coincided with substantial differences in the structural quality of the newly regenerated nerve. Indeed, near proximal regions exhibited increased macrophage and connective tissue infiltration as well as reduced epineurial and basal lamina integrity. Such

phenomena would be expected at the injury site itself, and thus may reflect either residual effects from the initial injury, or a gradual retrograde flow of inflammatory and fibrotic pathways from the exposed regenerating nerve front, which at 3 weeks was several mm from the near proximal region (Figure 9).

In the distal stump, we initially hypothesized that, based on consistent gross macroscopic appearance, nerves would reveal a similar regenerative environment. If anything, based on studies suggesting a poor regenerative environment in the far distal stump, near distal regions might be expected to offer a more favorable regenerative environment (Gordon, 2020). However, though both regions showed some laminar compaction consistent with Wallerian degeneration, there were dramatic differences in the inflammatory and structural environments between near and far distal stumps. Indeed, near distal stumps displayed increased connective tissue infiltration, a reduced laminar footprint, and reduced epineurial and laminar integrity. As also for the proximal stump, these observations likely reflect a gradual proximal to distal progression of inflammatory and fibrotic processes emerging from the site of nerve transection. Such
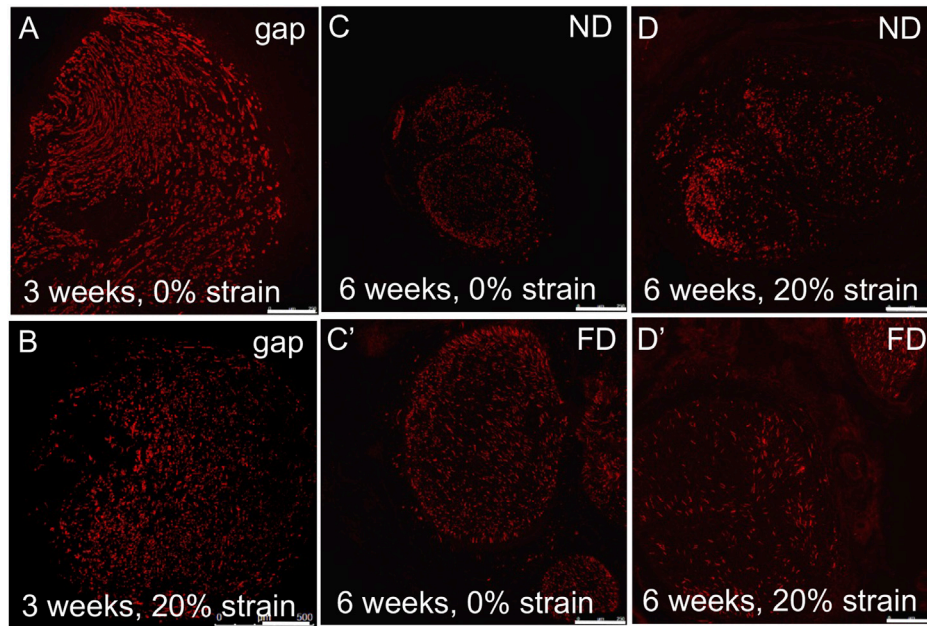
**FIGURE 9**
Axonal outgrowth into distal stump. **(A,B)** Axons (SMI-31 immunolabeling) grew into the PLGA conduit within 3 weeks after injury, irrespective of stretch. **(C,D/C',D')** Robust axonal growth was observed in **(C,D)** near distal stumps and **(C',D')** far distal stumps, irrespective of stretch, within 6 weeks after injury. These findings confirmed the feasibility of combining tension-based and conduit-based strategies for axonal regeneration. Scale bars: 100 μm.
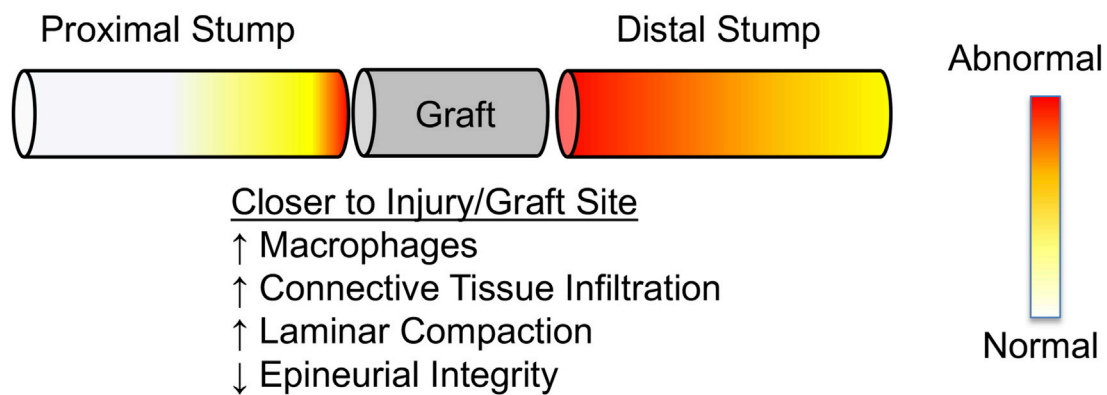


**FIGURE 10**
Schematic summarizing observed regional changes in nerve morphology near and far from the injury site. Proximity to injury/graft site results in more significant remodeling than regions away from the injury/graft site. Distal stumps appear to remodel further along their length than proximal stumps, consistent with Wallerian degeneration.

changes would be expected to have a dramatic negative influence on any axons just entering the distal stump, as they grow towards their targeted end organ. The clinical impacts of this finding are twofold. First, the initial trimming back, or "freshening," of the distal nerve stump by only a few mm during an initial repair, while providing a visually clean interface for securing a graft, may not, in fact, provide a favorable regenerative environment if the internal environment is not similarly "clean." This may provide one additional factor contributing to the poor response of a nerve to transection (Schmidt and Leach, 2003; Meek et al., 2005; Selim et al., 2022). Second, if this poor structural quality is indeed a result

of the initial injury, though counterintuitive, it may be beneficial to more aggressively trim the distal stump, to encourage axonal outgrowth into a more supportive environment. Tension-based strategies may offset this additional pruning.

## Limitations and implications for peripheral nerve regeneration

Our data support the use of nerve lengthening strategies for nerve regeneration. Nerves were successfully stretched using the device, and

stably maintained under loading without slippage. Axons also robustly regenerated through an integrated conduit. Given the lack of any adverse phenotypes, even by the most conservative interpretation of the data, lengthened nerves were provided a 2 mm (20%) head start in closing a 10 mm nerve gap, or a 4 mm (40%) head start if assessed based on the length of nerve removed from the gap (12 mm vs. 8 mm).

While we successfully assessed the quality of regenerating axons and their surrounding structural and inflammatory environment, a limitation of our study is that we did not compare functional regeneration due to our focus on nerve response at early time points. Per a number of prior studies, summarized in (Wood et al., 2011), functional assessments are likely to be most valuable at later time points of 3–4 months. Another limitation of our study was the observed partial collapse of several PLGA conduits mid-graft. While this did not affect the accuracy of our analysis or interpretation of our data, it did increase the variability and preclude the accurate quantification of axonal density and number mid-graft. Though PLGA has been successfully used to fabricate nerve regeneration scaffolds with modest structural and functional recovery (Oh and Lee, 2007; Oh et al., 2008), their biodegradability may render them fragile as well as elicit a local inflammatory response upon fragmentation (Chereddy et al., 2016). Thus, a more robust, non-tubular conduit such as an autologous graft or an acellular allograft may offer a more structurally sound alternative for longer gaps. Alternately, given the poor quality of the near distal stump noted above, proposed dynamic lengthening would accelerate gap closure, despite the need for follow-up freshening and end to end repair to anastomose clean interfaces. Previous studies have demonstrated the feasibility and potential benefits of lengthening the proximal stump beyond the edge of the distal stump, such that during device removal, nerve stumps are trimmed back and reattached at a single interface, in the absence of a graft (Vaz et al., 2014; Howarth et al., 2019b; Howarth et al., 2020). Overall, our work adds to mounting evidence that nerves can capably tolerate strain, and that nerve lengthening offers an attractive and novel approach to peripheral nerve repair.

## Data availability statement

The raw data supporting the conclusion of this article will be made available by the authors, without undue reservation.

## Ethics statement

The animal study was reviewed and approved by University of California, San Diego Institutional Animal Care and Use Committee.

## Author contributions

T-HC and SS designed experiments. T-HC and KV designed and executed experiments. T-HC, EO, JN, KV, RL, and SS analyzed data. T-HC and SS authored the initial manuscript draft. All authors reviewed and edited the manuscript.

## Acknowledgments

## Conflict of interest

The authors declare that the research was conducted in the absence of any commercial or financial relationships that could be construed as a potential conflict of interest.

## Publisher's note

All claims expressed in this article are solely those of the authors and do not necessarily represent those of their affiliated organizations, or those of the publisher, the editors and the reviewers. Any product that may be evaluated in this article, or claim that may be made by its manufacturer, is not guaranteed or endorsed by the publisher.

## References

Abrams, R. A., Butler, J. M., Bodine-Fowler, S., and Botte, M. J. (1998). Tensile properties of the neurorrhaphy site in the rat sciatic nerve. *J. Hand Surg. Am.* 23 (3), 465–470. doi:10.1016/s0363-5023(05)80464-2

Anava, S., Greenbaum, A., Jacob, E. B., Hanein, Y., and Ayali, A. (2009). The regulative role of neurite mechanical tension in network development. *Biophys. J.* 96 (4), 1661–1670. doi:10.1016/j.bpj.2008.10.058

Arnaoutoglou, C. M., Sakellariou, A., Vekris, M., Mitsionis, G. I., Korompilias, A., Ioakim, E., et al. (2006). Maximum intraoperative elongation of the rat sciatic nerve with tissue expander: Functional, neurophysiological, and histological assessment. *Microsurgery* 26 (4), 253–261. doi:10.1002/micr.20236

Asri, N. A. N., Mahat, M. M., Zakaria, A., Safian, M. F., and Abd Hamid, U. M. (2022). Fabrication methods of electroactive scaffold-based conducting polymers for tissue engineering application: A review. *Front. Bioeng. Biotechnol.* 10, 876696. doi:10.3389/fbioe.2022.876696

Bazarek, S., Brown, J. M., and Shah, S. B. (2022). Clinical potential of tension-lengthening strategies during nerve repair. *Neural Regen. Res.* 17 (4), 779–780. doi:10.4103/1673-5374.322461

Beris, A. E., Naka, K. K., Skopelitou, A., Kosta, I., Vragalas, V., Konitsiotis, S., et al. (1996). Functional assessment of the rat sciatic nerve following intraoperative expansion:

The effect of recovery duration on behavioural, neurophysiological, and morphological measures. *Microsurgery* 17 (10), 568–577. doi:10.1002/(sici)1098-2752(1996)17:10<568:aid-micr7>3.0.co;2-m

Bhatia, A., Doshi, P., Koul, A., Shah, V., Brown, J. M., and Salama, M. (2017). Contralateral C-7 transfer: Is direct repair really superior to grafting? *Neurosurg. Focus* 43 (1), E3. doi:10.3171/2017.4.focus1794

Birch, J. G., and Samchukov, M. L. (2004). Use of the Ilizarov method to correct lower limb deformities in children and adolescents. *J. Am. Acad. Orthop. Surg.* 12 (3), 144–154. doi:10.5435/00124635-200405000-00002

Bober, B. G., Gutierrez, E., Plaxe, S., Groisman, A., and Shah, S. B. (2015). Combinatorial influences of paclitaxel and strain on axonal transport. *Exp. Neurol.* 271, 358–367. doi:10.1016/j.expneurol.2015.06.023

Bray, D. (1984). Axonal growth in response to experimentally applied mechanical tension. *Dev. Biol.* 102 (2), 379–389. doi:10.1016/0012-1606(84)90202-1

Brown, J. M., Shah, M. N., and Mackinnon, S. E. (2009). Distal nerve transfers: A biology-based rationale. *Neurosurg. Focus* 26 (2), E12. doi:10.3171/foc.2009.26.2.e12

Brown, R., Pedowitz, R., Rydevik, B., Woo, S., Hargens, A., Massie, J., et al. (1993). Effects of acute graded strain on efferent conduction properties in the rabbit tibial

nerve. *Clin. Orthop. Relat. Res.* 296 (296), 288–294. doi:10.1097/00003086-199311000-00046

Carr, M. M., Best, T. J., Mackinnon, S. E., and Evans, P. J. (1992). Strain differences in autotomy in rats undergoing sciatic nerve transection or repair. *Ann. Plast. Surg.* 28 (6), 538–544. doi:10.1097/00000637-199228060-00008

Chereddy, K. K., Vandermeulen, G., and Preat, V. (2016). PLGA based drug delivery systems: Promising carriers for wound healing activity. *Wound Repair Regen.* 24 (2), 223–236. doi:10.1111/wrr.12404

Chuang, T. H., Wilson, R. E., Love, J. M., Fisher, J. P., and Shah, S. B. (2013). A novel internal fixator device for peripheral nerve regeneration. *Tissue Eng. Part C Methods* 19 (6), 427–437. doi:10.1089/ten.tec.2012.0021

de Assis, A. C. C., Reis, A. L. S., Nunes, L. V., Ferreira, L. F. R., Bilal, M., Iqbal, H. M. N., et al. (2022). Stem cells and tissue engineering-based therapeutic interventions: Promising strategies to improve peripheral nerve regeneration. *Cell Mol. Neurobiol.* doi:10.1007/s10571-022-01199-3

Dennerll, T. J., Lamoureux, P., Buxbaum, R. E., and Heidemann, S. R. (1989). The cytomechanics of axonal elongation and retraction. *J. Cell Biol.* 109 (6), 3073–3083. doi:10.1083/jcb.109.6.3073

Dunn, J. C., Tadlock, J., Klahs, K. J., Narimissaei, D., McKay, P., and Nesti, L. J. (2021). Nerve reconstruction using processed nerve allograft in the U.S. Military. *Mil. Med.* 186 (5-6), e543–e548. doi:10.1093/milmed/usaa494

Faul, F., Erdfelder, E., Lang, A. G., and Buchner, A. (2007). G*Power 3: A flexible statistical power analysis program for the social, behavioral, and biomedical sciences. *Behav. Res. Methods* 39 (2), 175–191. doi:10.3758/bf03193146

Flores, A. J., Lavernia, C. J., and Owens, P. W. (2000). Anatomy and physiology of peripheral nerve injury and repair. *Am. J. Orthop. (Belle Mead NJ)* 29 (3), 167–173.

Foran, I. M., Hussey, V., Patel, R. A., Sung, J., and Shah, S. B. (2017). Native paraneurial tissue and paraneurial adhesions alter nerve strain distribution in rat sciatic nerves. *J. Hand Surg.* 43(3):316–323. doi:10.1177/1753193417734433

Garg, S. P., Hassan, A. M., Patel, A. A., Perez, M. M., Stoehr, J. R., Ketheeswaran, S., et al. (2021). Outcomes of tibial nerve repair and transfer: A structured evidence-based systematic review and meta-analysis. *J. Foot Ankle Surg.* 60 (6), 1280–1289. doi:10.1053/j.jfas.2021.07.001

Geuna, S., Raimondo, S., Ronchi, G., Di Scipio, F., Tos, P., Czaja, K., et al. (2009). Chapter 3: Histology of the peripheral nerve and changes occurring during nerve regeneration. *Int. Rev. Neurobiol.* 87, 27–46. doi:10.1016/S0074-7742(09)87003-7

Gordon, T. (2020). Peripheral nerve regeneration and muscle reinnervation. *Int. J. Mol. Sci.* 21 (22), 8652. doi:10.3390/ijms21228652

Grinsell, D., and Keating, C. P. (2014). Peripheral nerve reconstruction after injury: A review of clinical and experimental therapies. *Biomed. Res. Int.* 2014, 1–13. doi:10.1155/2014/698256

Gupta, R., Rowshan, K., Chao, T., Mozaffar, T., and Steward, O. (2004). Chronic nerve compression induces local demyelination and remyelination in a rat model of carpal tunnel syndrome. *Exp. Neurol.* 187 (2), 500–508. doi:10.1016/j.expneurol.2004.02.009

Gupta, R., Nassiri, N., Hazel, A., Bathen, M., and Mozaffar, T. (2012). Chronic nerve compression alters Schwann cell myelin architecture in a murine model. *Muscle Nerve* 45 (2), 231–241. doi:10.1002/mus.22276

Hara, Y., Nishiura, Y., Ochiai, N., Sharula, Nakajima, Y., Kubota, S., et al. (2012). New treatment for peripheral nerve defects: Reconstruction of a 2?cm, monkey median nerve gap by direct lengthening of both nerve stumps. *J. Orthop. Res.* 30 (1), 153–161. doi:10.1002/jor.21476

Hentz, V. R., Rosen, J. M., Xiao, S. J., McGill, K. C., and Abraham, G. (1993). The nerve gap dilemma: A comparison of nerves repaired end to end under tension with nerve grafts in a primate model. *J. Hand Surg. Am.* 18 (3), 417–425. doi:10.1016/0363-5023(93)90084-g

Howarth, H. M., Alaziz, T., Nicolds, B., and O'Connor, S. (2019). Redistribution of nerve strain enables end-to-end repair under tension without inhibiting nerve regeneration. *Neural Regen. Res.* 14 (7), 1280–1288. doi:10.4103/1673-5374.251338

Howarth, H. M., Kadoor, A., Salem, R., Nicolds, B., Adachi, S., Kanaris, A., et al. (2019). Nerve lengthening and subsequent end-to-end repair yield more favourable outcomes compared with autograft repair of rat sciatic nerve defects. *J. Tissue Eng. Regen. Med.* 13 (12), 2266–2278. doi:10.1002/term.2980

Howarth, H. M., Orozco, E., Lovering, R. M., and Shah, S. B. (2020). A comparative assessment of lengthening followed by end-to-end repair and isograft repair of chronically injured peripheral nerves. *Exp. Neurol.* 331, 113328. doi:10.1016/j.expneurol.2020.113328

Jiang, B., Zhang, P., Yan, J., and Zhang, H. (2008). Dynamic observation of biomechanic properties of sciatic nerve at the suture site in rats following repairing. *Artif. Cells Blood Substit. Immobil. Biotechnol.* 36 (1), 45–50. doi:10.1080/10731190701857777

Kechele, P. R., Bertelli, J. A., Dalmarco, E. M., and Frode, T. S. (2011). The mesh repair: Tension free alternative on dealing with nerve gaps-experimental results. *Microsurgery* 31 (7), 551–558. doi:10.1002/micr.20902

Li, Y., Ma, Z., Ren, Y., Lu, D., Li, T., Li, W., et al. (2021). Tissue engineering strategies for peripheral nerve regeneration. *Front. Neurol.* 12, 768267. doi:10.3389/fneur.2021.768267

Loverde, J. R., Ozoka, V. C., Aquino, R., Lin, L., and Pfister, B. J. (2011). Live imaging of axon stretch growth in embryonic and adult neurons. *J. Neurotrauma* 28 (11), 2389–2403. doi:10.1089/neu.2010.1598

Loverde, J. R., and Pfister, B. J. (2015). Developmental axon stretch stimulates neuron growth while maintaining normal electrical activity, intracellular calcium flux, and somatic morphology. *Front. Cell Neurosci.* 9, 308. doi:10.3389/fncel.2015.00308

Lundborg, G., and Rydevik, B. (1973). Effects of stretching the tibial nerve of the rabbit. A preliminary study of the intraneural circulation and the barrier function of the perineurium. *J. Bone Jt. Surg. Br.* 55 (2), 390–401. doi:10.1302/0301-620x.55b2.390

Maeda, T., Hori, S., Sasaki, S., and Maruo, S. (1999). Effects of tension at the site of coaptation on recovery of sciatic nerve function after neurorrhaphy: Evaluation by walking-track measurement, electrophysiology, histomorphometry, and electron probe X-ray microanalysis. *Microsurgery* 19 (4), 200–207. doi:10.1002/(sici)1098-2752(1999)19:4<200:aid-micr7>3.0.co;2-y

Maeng, W. Y., Tseng, W.-L., Li, S., Koo, J., and Hsueh, Y-Y. (2022). Electroceuticals for peripheral nerve regeneration. *Biofabrication* 14. doi:10.1088/1758-5090/ac8baa

Mason, S., and Phillips, J. B. (2011). An ultrastructural and biochemical analysis of collagen in rat peripheral nerves: The relationship between fibril diameter and mechanical properties. *J. Peripher. Nerv. Syst.* 16 (3), 261–269. doi:10.1111/j.1529-8027.2011.00352.x

Meek, M. F., Coert, J. H., and Robinson, P. H. (2005). Poor results after nerve grafting in the upper extremity: Quo vadis? *Microsurgery* 25 (5), 396–402. doi:10.1002/micr.20137

Millesi, H. (1981). Reappraisal of nerve repair. *Surg. Clin. North Am.* 61 (2), 321–340. doi:10.1016/s0039-6109(16)42384-4

Millesi, H. (1986). The nerve gap. *Hand Clin.* 2 (4), 651–663. doi:10.1016/s0749-0712(21)00614-4

Mueller, M. J., and Maluf, K. S. (2002). Tissue adaptation to physical stress: A proposed "physical stress theory" to guide physical therapist practice, education, and research. *Phys. Ther.* 82 (4), 383–403. doi:10.1093/ptj/82.4.383

Ogata, K., and Naito, M. (1986). Blood flow of peripheral nerve effects of dissection, stretching and compression. *J. Hand Surg. Br.* 11 (1), 10–14. doi:10.1016/0266-7681_86_90003-3

Oh, S. H., Kim, J. H., Song, K. S., Jeon, B. H., Yoon, J. H., Seo, T. B., et al. (2008). Peripheral nerve regeneration within an asymmetrically porous PLGA/Pluronic F127 nerve guide conduit. *Biomaterials* 29 (11), 1601–1609. doi:10.1016/j.biomaterials.2007.11.036

Oh, S. H., and Lee, J. H. (2007). Fabrication and characterization of hydrophilized porous PLGA nerve guide conduits by a modified immersion precipitation method. *J. Biomed. Mater. Res. A* 80 (3), 530–538. doi:10.1002/jbm.a.30937

Peters, B. R., Wood, M. D., Hunter, D. A., and Mackinnon, S. E. (2021). Acellular nerve allografts in major peripheral nerve repairs: An analysis of cases presenting with limited recovery. *Hand (N Y)*, 15589447211003175. doi:10.1177/15589447211003175

Pfister, B. J., Iwata, A., Meaney, D. F., and Smith, D. H. (2004). Extreme stretch growth of integrated axons. *J. Neurosci.* 24 (36), 7978–7983. doi:10.1523/jneurosci.1974-04.2004

Phillips, J. B., Smit, X., Zoysa, N. D., Afoke, A., and Brown, R. A. (2004). Peripheral nerves in the rat exhibit localized heterogeneity of tensile properties during limb movement. *J. Physiol.* 557 (3), 879–887. doi:10.1113/jphysiol.2004.061804

Poongodi, R., Chen, Y. L., Yang, T. H., Huang, Y. H., Yang, K. D., Lin, H. C., et al. (2021). Bio-scaffolds as cell or exosome carriers for nerve injury repair. *Int. J. Mol. Sci.* 22 (24), 13347. doi:10.3390/ijms222413347

Ray, C. D., and Maurer, D. D. (1975). Electrical neurological stimulation systems: A review of contemporary methodology. *Surg. Neurol.* 4 (1), 82–90.

Rbia, N., Bulstra, L. F., Saffari, T. M., Hovius, S. E., and Shin, A. Y. (2019). Collagen nerve conduits and processed nerve allografts for the reconstruction of digital nerve gaps: A single-institution case series and review of the literature. *World Neurosurg.* 127, e1176–e1184. doi:10.1016/j.wneu.2019.04.087

Safa, B., Jain, S., Desai, M. J., Greenberg, J. A., Niacaris, T. R., Nydick, J. A., et al. (2020). Peripheral nerve repair throughout the body with processed nerve allografts: Results from a large multicenter study. *Microsurgery* 40 (5), 527–537. doi:10.1002/micr.30574

Saijilafu, Nishiura, Y., Yamada, Y., Hara, Y., Ichimura, H., Yoshii, Y., et al. (2006). Repair of peripheral nerve defect with direct gradual lengthening of the proximal nerve stump in rats. *J. Orthop. Res.* 24 (12), 2246–2253. doi:10.1002/jor.20280

Schmidt, C. E., and Leach, J. B. (2003). Neural tissue engineering: Strategies for repair and regeneration. *Annu. Rev. Biomed. Eng.* 5, 293–347. doi:10.1146/annurev.bioeng.5.011303.120731

Selim, O. A., Lakhani, S., Midha, S., Mosahebi, A., and Kalaskar, D. M. (2022). Three-dimensional engineered peripheral nerve: Toward a new era of patient-specific nerve repair solutions. *Tissue Eng. Part B Rev.* 28 (2), 295–335. doi:10.1089/ten.teb.2020.0355

Sharula, Hara, Y., Nishiura, Y., Saijilafu, Kubota, S., and Ochiai, N. (2010). Repair of the sciatic nerve defect with a direct gradual lengthening of proximal and distal nerve stumps in rabbits. *Plast. Reconstr. Surg.* 125 (3), 846–854. doi:10.1097/prs.0b013e3181ccdbd4

Siechen, S., Yang, S., Chiba, A., and Saif, T. (2009). Mechanical tension contributes to clustering of neurotransmitter vesicles at presynaptic terminals. *Proc. Natl. Acad. Sci. U. S. A.* 106 (31), 12611–12616. doi:10.1073/pnas.0901867106

Simpson, A. H., Gillingwater, T. H., Anderson, H., Cottrell, D., Sherman, D. L., Ribchester, R. R., et al. (2013). Effect of limb lengthening on internodal length and conduction velocity of peripheral nerve. *J. Neurosci.* 33 (10), 4536–4539. doi:10.1523/jneurosci.4176-12.2013

Singh, V. K., Haq, A., Tiwari, M., and Saxena, A. K. (2022). Approach to management of nerve gaps in peripheral nerve injuries. *Injury* 53 (4), 1308–1318. doi:10.1016/j.injury.2022.01.031

Sunderland, I. R., Brenner, M. J., Singham, J., Rickman, S. R., Hunter, D. A., and Mackinnon, S. E. (2004). Effect of tension on nerve regeneration in rat sciatic nerve transection model. *Ann. Plast. Surg.* 53 (4), 382–387. doi:10.1097/01.sap.0000125502.63302.47

Sung, J., Sikora-Klak, J., Adachi, S. Y., Orozco, E., and Shah, S. B. (2019). Decoupled epineurial and axonal deformation in mouse median and ulnar nerves. *Muscle Nerve* 59 (5), 619–628. doi:10.1002/mus.26437

Tanoue, M., Yamaga, M., Ide, J., and Takagi, K. (1996). Acute stretching of peripheral nerves inhibits retrograde axonal transport. *J. Hand Surg. Br.* 21 (3), 358–363. doi:10.1016/s0266-7681(05)80203-7

Vaz, K. M., Brown, J. M., and Shah, S. B. (2014). Peripheral nerve lengthening as a regenerative strategy. *Neural Regen. Res.* 9 (16), 1498–1501. doi:10.4103/1673-5374.139471

Wall, E. J., Massie, J., Kwan, M., Rydevik, B., Myers, R., and Garfin, S. R. (1992). Experimental stretch neuropathy. Changes in nerve conduction under tension. *J. Bone Jt. Surg. Br.* 74 (1), 126–129. doi:10.1302/0301-620x.74b1.1732240

Wood, M. D., Kemp, S. W., Weber, C., Borschel, G. H., and Gordon, T. (2011). Outcome measures of peripheral nerve regeneration. *Ann. Anat.* 193 (4), 321–333. doi:10.1016/j.aanat.2011.04.008

Wright, T. W., Glowczewskie, F., Cowin, D., and Wheeler, D. L. (2001). Ulnar nerve excursion and strain at the elbow and wrist associated with upper extremity motion. *J. Hand Surg. Am.* 26 (4), 655–662. doi:10.1053/jhsu.2001.26140

Yousef, M. A., Dionigi, P., Marconi, S., Calligaro, A., Cornaglia, A. I., Alfonsi, E., et al. (2015). Successful reconstruction of nerve defects using distraction neurogenesis with a new experimental device. *Basic Clin. Neurosci.* 6 (4), 253–264.

Zeng, Z., Yang, Y., Deng, J., Saif Ur Rahman, M., Sun, C., and Xu, S. (2022). Physical stimulation combined with biomaterials promotes peripheral nerve injury repair. *Bioeng. (Basel)* 9 (7), 292. doi:10.3390/bioengineering9070292

Zheng, J., Lamoureux, P., Santiago, V., Dennerll, T., Buxbaum, R., and Heidemann, S. (1991). Tensile regulation of axonal elongation and initiation. *J. Neurosci.* 11 (4), 1117–1125. doi:10.1523/jneurosci.11-04-01117.1991